Published in final edited form as:
Free Radic Biol Med. 2010 December 1; 49(11): 1674–1684. doi:10.1016/j.freeradbiomed.2010.08.028.

Neuroprotection by a mitochondria-targeted drug in a Parkinson's disease model

Anamitra Ghosh[a], **Karunakaran Chandran**[b,1], **Shasi V. Kalivendi**[b,2], **Joy Joseph**[b], **William E. Antholine**[b], **Cecilia J. Hillard**[c], **Arthi Kanthasamy**[a], **Anumantha Kanthasamy**[a], and **Balaraman Kalyanaraman**[b,*]

[a]Department of Biomedical Sciences, College of Veterinary Medicine, Iowa State University, Ames, IA 50011, USA

[b]Department of Biophysics, Medical College of Wisconsin, Milwaukee, WI 53226, USA

[c]Department of Pharmacology & Toxicology, Medical College of Wisconsin, Milwaukee, WI 53226, USA

Abstract

The objective of this study was to assess the neuroprotective effects of a mitochondria-targeted antioxidant, Mito-Q_{10}, the coenzyme-Q analog attached to a triphenylphosphonium cation that targets the antioxidant to mitochondria, in experimental models of Parkinson's disease (PD). Primary mesencephalic neuronal cells and cultured dopaminergic cells were treated with 1-methyl-4-phenylpyridinium (MPP^+), an active metabolite of the neurotoxin 1-methyl-4-phenyl-1,2,3,6-tetrahydropyridine (MPTP), and mice were used for testing the efficacy of Mito-Q_{10}. MPP^+ treatment caused a dose-dependent loss of tyrosine hydroxylase and membrane potential and an increase in caspase-3 activation in dopaminergic cells, which were reversed by Mito-Q_{10}. MPTP treatment induced a loss of striatal dopamine and its metabolites, inactivation of mitochondrial aconitase in the substantia nigra, and a loss of locomotor activity in mice. Treatment with Mito-Q_{10} significantly inhibited both MPP^+- and MPTP-induced neurotoxicity in cell culture and mouse models. Collectively, these results indicate that mitochondrial targeting of antioxidants is a promising neuroprotective strategy in this preclinical mouse model of PD.

Keywords

MPTP; MPP^+; Mito-Q_{10}; Co-Q; Parkinson's disease; Oxidants; Oxidative stress; Free radicals

*Corresponding author. Department of Biophysics, Medical College of Wisconsin, 8701 Watertown Plank Road, Miwaukee, WI 53226, USA. Fax: +1 414 456 6512. balarama@mcw.edu (B. Kalyanaraman).
[1]Present address: Biomedical Research Lab, VHNSN College, Virudhunagar-626001, TN, India.
[2]Present address: Center for Chemical Biology (Org-1), Indian Institute of Chemical Technology, Uppal Road, Hyderabad 500 007, India.

Supplementary data associated with this article can be found in the online version at doi:10.1016/j.freeradbiomed.2010.08.028.

Introduction

The degeneration of mesencephalic dopamine neurons (MDNs)[3] is central to the onset of Parkinson's disease (PD) [1,2]. Mitochondrial dysfunction and oxidative stress are mainly responsible for the MDN degeneration in PD [2]. Patients suffering from PD exhibit a defective neuronal mitochondrial function and deficiency of the neurotransmitter dopamine [3,4]. Epidemiological studies strongly suggest a link between mitochondrial toxins (e.g., rotenone) and the etiology of PD [5]. A commonly used preclinical animal model of PD is the 1-methyl-4-phenyl-1,2,3,6-tetrahydropyridine (MPTP) model [6,7]. MPTP, a contaminant of an illicit narcotic, induces PD-like symptoms in experimental animals [1,8,9]. Although the MPTP model of PD differs from idiopathic PD, there are many biochemical and pathological similarities, including selective destruction of dopaminergic neurons in the substantia nigra (SN) [10–12]. The ultimate toxic metabolite, 1-methyl-4-phenylpyridinium (MPP^+), is formed by monoamine oxidase (type B)-catalyzed oxidation of MPTP [13,14]. The MPP^+ transported into the dopaminergic neurons by the dopamine transporter accumulates in the mitochondria, resulting in adenosine triphosphate depletion through inhibition of complex I activity, altered mitochondrial membrane potential, increased reactive oxygen species (ROS), and apoptotic cell death [15,16]. Systemic inhibition of complex I activity was shown to cause parkinsonism in other animal models, reproducing the features of PD [12,17–19].

Many neurodegenerative diseases are associated with mitochondrial dysfunction [20,21]. Defects in complexes I, II, and IV of the mitochondrial respiratory chain have been detected in Alzheimer's, Parkinson's, and Huntington's diseases. Several lines of evidence implicate PD as a free radical disease involving mitochondrial dysfunction leading to energy failure [22]. Increased oxidative damage, dopamine depletion, protein nitration, iron accumulation, protein aggregation, and apoptosis are all characteristic hallmarks of PD [23,24]. Numerous antioxidants and iron chelators have been utilized in PD animal models with partial success [25–27]. Mitochondria-targeted antioxidants (MTAs) have not yet been used in PD animal models. MTAs were shown to be more potent than "untargeted" parent antioxidants in endothelial cells subjected to oxidant stress [28]. Recent research has shown that the mitochondrial uptake of antioxidants (vitamin E, coenzyme-Q) coupled to a triphenylphosphonium cation (Mito-E, Mito-Q_{10}) is facilitated by the large negative membrane potential across the mitochondrial inner membrane [29]. Here we tested the neuroprotective efficacy of Mito-Q_{10} in response to MPP^+/MPTP treatment in neuronal cell culture systems and in a preclinical mouse model of PD. Results show that Mito-Q_{10} treatment affords neuroprotection in these model systems.

Materials and methods

Materials

1-Methyl-4-phenylpyridinium ion (MPP^+ iodide), 3-(4,5-dimethylthiazol-2-yl)-2,5-diphenyltetrazolium bromide (MTT), α-methyl-*p*-tyrosine, and MPTP–HCl were purchased from Sigma (St. Louis, MO, USA). The fluorogenic substrates for caspase assay Ac-DEVD-AFC (caspase-3 substrate) and Ac-LEHD-AFC (caspase-9 strate) were purchased from

EMD (San Diego, CA, USA). Mito-Q_{10} and Mito-undecanol (Mito-Q without the ubiquinone/ubiquinol moiety) were synthesized as previously reported [30].

Cell cultures

Primary cultures of rat MDNs were established according to previously published methods [31]. Briefly, neurons from the ventral mesencephalon of rat embryos on the 16th day of gestation were dissociated mechanically, and after treatment with trypsin (0.2 mg/ml) and deoxyribonuclease (40 mg/ml), cells were plated onto 0.1% poly-D-lysine-coated six-well plates at a density of 1.1×10^5 cells/cm^2. Cells were cultured in Neurobasal medium (Invitrogen, Carlsbad, CA, USA) with 2% (vol/vol) B27 supplement (Invitrogen) for 6 days. Animals were treated in accordance with the guidelines published in the NIH *Guide for the Care and Use of Laboratory Animals.*

The N27 cell line derived from rat MDNs [32,33] was also used in this study. Briefly, cells were maintained in Dulbecco's modified Eagle's medium (DMEM) containing 10% fetal bovine serum (FBS) in the presence of penicillin, streptomycin, and glutamine as described previously [34]. Twelve hours before treatments, the medium was replaced with DMEM containing 2% FBS.

Cell viability

Intracellular conversion of MTT to formazan was used as an indicator of cell viability (λ_{max} =560 nm). After treatments, the culture media were removed, the cells were washed twice with serum-free DMEM, and the cells were incubated with MTT (0.25 mg/ml DMEM). After a 2-h incubation, cell viability was assessed as described previously [35].

The optimal MTA concentration was determined by monitoring their dose–response cytotoxic effects, using the Sytox assay in N27 cells. After treatments with MPP^+ at various concentrations, the cell culture media were removed and cells were washed twice with serum-free DMEM and incubated with Sytox (0.25 mg/ml). The cytotoxicity was assessed by monitoring the Sytox green fluorescence using a Gemini fluorescence plate reader (ex 485 nm, em 538 nm). Fluorescence images of Sytox-positive cells were captured with a SPOT digital camera attached to a Nikon TE200 microscope.

Caspase activity measurements

Caspase-3- and caspase-9-like activities were measured as described previously [36]. Briefly, cells were suspended in 100 μl of lysis buffer (Sigma) and passed through a 24-gauge needle 10 times to ensure complete lysis. The lysate was centrifuged at 4 °C for 10 min at 10,000 rpm, and 50 μl of the clear supernatant was used for the activity assay, according to the manufacturer's protocol. The increase in the fluorescence (ex 405 nm, em 500 nm) was considered an index of caspase activity.

Immunoblotting

After treatments, cells were washed with DPBS and resuspended in 100 μl of radioimmune precipitation buffer (20 mM Tris–HCl, pH 7.4, 2.5 mM EDTA, 1% Triton X-100, 1% sodium deoxycholate, 1% SDS, 100 mM NaCl, 100 mM sodium fluoride) containing a

protease inhibitor cocktail (Roche, Basel, Switzerland). Protein concentrations were determined by the Lowry method (Bio-Rad, Hercules, CA, USA) and proteins (40 μg) were resolved by 10% SDS–PAGE and blots were developed as described previously [36]. Monoclonal antibodies against tyrosine hydroxylase (TH; Cell Signaling, Danvers, MA, USA) and β-actin (Millipore, Billerica, MA, USA) were employed to detect TH and β-actin, respectively.

Tyrosine hydroxylase (TH) immunocytochemistry

After the termination of incubation, cells were washed once with DPBS and fixed (3% paraformaldehyde, 0.02% glutaraldehyde in PBS) for 15 min at room temperature. Cells were then permeabilized by dipping for 10 s in 100% methanol (−20 °C) and then incubated three times for 10 min each with 0.5 mg/ml $NaBH_4$ in PBS, pH 8.0, to reduce the aldehyde groups, and then rinsed with PBS three times, 5 min each. Cells were permeabilized with 0.01% Triton X-100 in PBS for 30 s and again washed with PBS three times, 5 min each. Cells were incubated in 1% bovine serum albumin (BSA) in PBS at pH 7.5 for 30 min to block any nonspecific binding of the antibodies and treated with TH primary antibody (polyclonal; Cell Signaling) in PBS (pH 7.5) containing 1% BSA and 0.1% saponin for 24 h. The cells were washed with PBS at pH 7.5, three times for 10 min each, and incubated for 120 min with FITC-labeled secondary antibody (Millipore) in PBS (pH 7.5) containing 1% BSA and 0.1% saponin at room temperature. Finally, the cells were washed three times for 10 min each with PBS and immediately observed under a fluorescence microscope (Nikon, Melville, NY, USA) equipped with FITC filter settings.

Diaminobenzidine immunostaining and stereological counting of TH-positive neurons

Tyrosine hydroxylase–diaminobenzidine (DAB) immunostaining was performed in striatal and substantia nigral sections as described previously [37]. Briefly, 7 days after the last dose of MPTP, mice were sacrificed and perfused with 4% paraformaldehyde (PFA) and postfixed with PFA and 30% sucrose. The fixed brains were subsequently cut using a cryostat into 30-μm coronal sections and kept in 30% sucrose–ethylene glycol solution at −20 °C. On the day of staining, sections were rinsed with PBS and incubated with the antiTH antibody (Calbiochem rabbit anti-mouse, 1:1600) overnight at 4 °C. Biotinylated anti-rabbit secondary antibody was used for 1 h at room temperature. The sections were then incubated with avidin peroxidase (Vectastatin ABC Elite kit) for 30 min at room temperature. Immunolabeling was observed using DAB, which yielded a brown stain. Total numbers of TH-stained neurons in SNpc were counted stereologically with Stereo Investigator software (Micro-BrightField, Williston, VT, USA), using an optical fractionator [37,38].

Mitochondrial membrane potential

The lipophilic dye JC-1 (Invitrogen) was used to measure the mitochondrial membrane potential. In healthy cells with intact membrane potential JC-1 forms aggregates, producing an intense orange signal. In apoptotic cells with collapsed mitochondrial membrane potential, JC-1 remains monomeric and stains the cytosol green. After termination of the experiment, cells were incubated for 30 min with JC-1 and washed twice with PBS. The proportion of aggregated versus monomeric JC-1 probe was quantified by measuring the

ratio of fluorescence emissions at 590 nm (orange) over 530 nm (green) in a Nikon fluorescence microscope equipped with Metamorph software.

HPLC analysis of striatal dopamine and its metabolite levels

The striatal dopamine (DA), 3,4-dihydroxyphenylacetic acid (DOPAC), and homovanillic acid (HVA) levels were quantified using high-performance liquid chromatography (HPLC) with electrochemical detection. Samples were prepared and quantified as described previously [33,39]. Briefly, after 7 days of MPTP injection, mice were sacrificed in a CO_2 chamber and striata were collected and stored at −80 °C. On the day of analysis, neurotransmitters from striatal tissues were extracted in 0.1 M perchloric acid solutions containing 0.05% Na_2EDTA and 0.1% $Na_2S_2O_5$ and isoproterenol (as an internal standard). The extracts were filtered in 0.22-μm spin tubes, and 20 μl of the sample was loaded for analysis. DA, DOPAC, and HVA were separated isocratically in a reversed-phase column using a flow rate of 0.7 ml/min. An HPLC system (ESA, Bedford, MA, USA) with an automatic sampler equipped with a refrigerated temperature control (Model 542; ESA) was used in these experiments. The electrochemical detection system consisted of a Coulochem Model 5100A with a microanalysis cell (Model 5014A) and a guard cell (Model 5020; ESA). Standard stock solutions of catecholamines (1 mg/ml) were prepared in perchloric acid solution and further diluted to a final working concentration of 50 pg/μl before injection. The data acquisition and analysis were performed using the EZStart HPLC software (ESA).

Animals and treatment

Six- to 8-week-old male C57BL/6 mice weighing 24 to 28 g were housed under standard conditions: constant temperature (22±1 °C) and humidity (relative, 30%) and a 12-h light/dark cycle. Mice were allowed free access to food and water. Use of the animals and protocol procedures were approved and supervised by the Committee on Animal Care at Iowa State University (Ames, IA, USA). Mice received Mito-Q_{10} (4 mg/kg dose) by oral gavage for 1 day (pretreatment before MPTP administration), 5 days (cotreatment with MPTP), and 7 days (post-treatment with MPTP). In the subacute MPTP regimens, MPTP (25 mg/kg) was injected intraperitoneally via a single dose daily starting on day 2 for 5 days. The control mice received saline at the same dose. Mito-Q_{10} was synthesized according to a modified procedure of a published method [40].

Behavioral measurements

In our experiment, two types of behavioral tests were performed, which included an open-field experiment for testing locomotor activities and the rotarod experiment to test foot movement of the mice after MPTP and Mito-Q_{10} treatments [33,39]. An automated device (AccuScan, Model RXYZCM-16; Columbus, OH, USA) was used to measure the spontaneous activity of the mice. The activity chamber was 40×40×30.5 cm, made of clear Plexiglas, and covered with a Plexiglas lid with holes for ventilation. The infrared monitoring sensors were located every 2.54 cm along the perimeter (16 infrared beams along each side) and 2.5 cm above the floor. Two additional sets of 16 sensors were located 8.0 cm above the floor on opposite sides. Data were collected and analyzed by a VersaMax analyzer (AccuScan, Model CDA-8). Before any treatment, mice were placed inside the

infrared monitor for 10 min daily for 3 consecutive days to train them. Five days after the last MPTP injection, both open-field and rotarod experiments were conducted. The locomotor activities are presented as horizontal movement, vertical movement, total distance traveled (cm), total movement time (s), total rest time (s), and rearing activity over a 10-min test session. For rotarod experiments, a speed of 20 rpm was used. Mice were given a 5- to 7-min rest interval to eliminate stress and fatigue.

EPR measurements

The X-band EPR of cortex, cerebellum, striatum, and substantial nigral tissues isolated from mouse brains were recorded at liquid helium temperatures on a Bruker BioSpin (Newton, MA, USA) E500 ELEXYS spectrometer with a 100-kHz field modulation, equipped with an Oxford Instruments (Tubney Woods, Abingdon, Oxfordshire, UK) helium flow cryostat and a DM-0101 cavity. Brain tissues were excised and immersed in liquid nitrogen and subsequently transferred to 4-mm quartz EPR tubes (Wilmad, Vineland, NJ, USA). The volume of the tissue sample in the EPR tube was always greater than the working zone of the cavity. Reloading of tissues in the same EPR tubes resulted in EPR spectra with a 5% variation in signal intensity [41]. Other spectrometer conditions were microwave frequency, 9.635 GHz; modulation amplitude, 4–10 G; and microwave power, 5 mW. EPR spectra were recorded over a temperature range of 4–50 K. Double integrations of experimental EPR spectra were performed using the copper EDTA standard. The microwave power dependence of each signal was analyzed as previously described [41].

Statistical analysis

Unpaired *t* tests were used for comparisons between groups, and Pearson correlations were performed between dependent variables using the statistical package Sigmastat (Ashburn, VA, USA). $P<0.05$ was considered significant.

Results

Mito-Q_{10} supplementation attenuates decrease in tyrosine hydroxylase levels and mitochondrial membrane potential in MPP^+-treated neuronal cells

We used both primary mesencephalic neuronal cultures and immortalized dopaminergic neuronal cells (N27 cells) for these experiments. As MDNs consist of neurons representing not more than 4–5% of dopamine neurons, we investigated the effects of Mito-Q_{10} using the N27 dopaminergic cell model. We and others have shown that this cell model shares many of the common properties associated with primary cultures of dopamine neurons [34,42,43]. MDNs were treated with various concentrations of MPP^+ for 48 h, and TH levels were determined by Western blotting. As shown in Fig. 1A (top and bottom), MPP^+ caused a dose-dependent decrease in TH protein levels. The survival of the dopamine neurons in MDNs was visualized by immunohistochemistry using the polyclonal antibodies raised against TH and a secondary antibody coupled to FITC (Fig. 1B). The loss of TH seen by immunoblotting of MDNs showed the same trend as determined for TH protein levels (Figs. 1A and 1C). Pretreatment of MDNs with Mito-Q_{10} (10 μM) restored MPP^+-induced loss of TH staining from 60 to 10% of control (Fig. 1D) (densitometric data not shown). The cytotoxicity of Mito-Q_{10} at several concentrations (1–100 μM) was examined in N27 cells.

Mito-Q_{10} was toxic at concentrations of ≈30 μM as determined by the Sytox method (not shown). Previously, it has been reported that Mito-Q_{10} causes endothelial cell toxicity at higher concentrations (≈100 μM) because of enhanced generation of superoxide [44].

The loss of mitochondrial membrane potential in response to MPP^+ treatment in N27 cells is shown in Fig. 2. N27 cells were incubated with MPP^+ in the presence and absence of Mito-Q_{10} for 48 h. The loss of mitochondrial membrane potential under these conditions was measured by staining with JC-1 (Mitosensor dye; Figs. 2A and 2B), a cationic dye that fluoresces differently in cells with normal and impaired mitochondria. The Mitosensor dye forms aggregates in mitochondria of healthy cells and exhibits red fluorescence. When membrane potentials are altered, this dye cannot accumulate in the mitochondria and remains as monomers, leading to a green fluorescence. After treatment with MPP^+ and MPP^+ plus Mito-Q_{10}, cells were treated for 30 min with JC-1 and washed twice with PBS, and the fluorescence images obtained under FITC and rhodamine filter settings were overlaid. The number of cells demonstrating aggregated vs monomeric JC-1 probe was quantified by measuring the ratio between the fluorescence emission at 580 (orange) and 530 nm (green) in a Nikon fluorescence microscope equipped with Metamorph software. Pre-treatment with Mito-Q_{10} significantly suppressed the loss of mitochondrial membrane potential as measured by JC-1 staining (Fig. 2).

MPP^+-induced cytotoxicity was determined by the Sytox method and by measuring caspase activation. The Sytox method labels only the nuclei of dead cells, yielding green fluorescence. N27 cells were incubated with MPP^+ (150 μM) for 24 h, and cell death and caspase activities were measured. As shown in Figs. 3A and 3B, MPP^+ treatment caused a two- to threefold increase in cell death. Pretreatment with Mito-Q_{10} for 2 h significantly inhibited MPP^+-induced cell death. Under these conditions, MPP^+ alone caused a six- to sevenfold increase in caspase-3 activation compared to control (Fig. 3C). Mito-Q_{10} pretreatment significantly decreased MPP^+-induced caspase-3 activation. These results suggest that mitochondria-generated oxidants may be involved in MPP^+-mediated apoptotic cell death in neuronal cells and that Mito-Q_{10} pretreatment counteracted MPP^+ neurotoxicity. Significant increases in caspase-9- and caspase-3-like activities were evident after a 36-h treatment with MPP^+ (10 μM) that increased up to 48 h (not shown). These results indicate that exposure to 10 μM MPP^+ is sufficient to induce apoptosis in MDNs and that the loss of TH paralleled the onset of apoptosis. Pretreatment of MDNs with Mito-Q_{10} inhibited the effect of MPP^+ to reduce protein levels of cellular TH (Fig. 1C) and caspase-3 activation (Fig. 3C). In contrast, pretreatment with Co-Q was not as effective (Fig. 3D).

Mito-Q_{10} inhibits MPP^+-induced decrease in dopamine levels

Next we monitored the effects of Mito-Q_{10} on alterations in dopamine levels in MDN cultures. MPP^+ caused a dose-dependent reduction in the cellular dopamine levels, with 10 μM MPP^+ causing nearly a twofold decrease by the end of 48 h treatment (Fig. 4A). Pretreatment of MDNs with Mito-Q_{10} (50 nM) restored the cellular dopamine levels to those observed in control MDNs (Fig. 4B).

Mito-Q_{10} attenuates depletion of dopamine and its metabolites induced by MPTP toxicity

After establishing that Mito-Q_{10} affords neuroprotection in a cell culture model, we investigated whether Mito-Q_{10} could inhibit depletion of dopamine and its metabolites in MPTP-treated mice. Mice were treated with Mito-Q_{10} (4 mg/kg) via oral gavage 1 day before MPTP administration, and treatment continued for another 12 days, according to the experimental protocols described under Materials and methods. MPTP (25 mg/kg) was administered intraperitoneally daily from day 2 to 7 (total five doses with a single dose per day), and after 7 days of MPTP treatment the mice were sacrificed and striatal tissues were processed for dopamine, DOPAC, and HVA measurements. As shown in Fig. 5A, MPTP administration led to a nearly 80% decrease in dopamine levels compared to control mice. Interestingly, MPTP-treated mice that also received Mito-Q_{10} showed only a 40–45% decrease in dopamine levels (Fig. 5A). Similarly, MPTP treatment inhibited DOPAC and HVA levels and pretreatment with Mito-Q_{10} significantly restored their levels (Figs. 5B and 5C).

To determine whether Mito-Q_{10} interferes with dopamine metabolism, we measured dopamine and its metabolite DOPAC in Mito-Q_{10}-treated mice. As shown in Supplementary Figs. S1C and S1D, we did not observe any significant difference in the amount of striatal dopamine and DOPAC between control and Mito-Q_{10}-treated mice. These results also suggest that Mito-Q_{10} does not interfere with MPTP metabolism because monoamine oxidase is the major enzyme responsible for conversion of MPTP to its toxic metabolite MPP^+.

Mito-Q_{10} protects the nigrostriatal axis against MPTP toxicity

As Mito-Q_{10} significantly restored striatal neurotransmitter levels in response to MPTP toxicity, we sought to determine whether Mito-Q_{10} could protect the nigrostriatum against MPTP toxicity. MPTP intoxication decreased the TH-positive neurons (Figs. 6B and 6C) and TH-positive terminals in striatum (Fig. 6A). Additionally, the stereological count of SNpc TH-positive neurons also showed a 65–70% loss of TH-positive neurons in MPTP-treated mice. Interestingly, there was less reduction of TH-positive fibers and neurons in striatum and substantia nigra in MPTP-injected mice in the presence of Mito-Q_{10} (Figs. 6A, 6B, and 6C). The stereological count of TH-positive neurons in SNpc also showed only a 25–30% loss of TH-positive neurons in MPTP-treated mice that received Mito-Q_{10} (Fig. 6D). Higher magnification (10×) pictures of the substantia nigra region showed that MPTP treatment resulted in a loss of TH-positive dopaminergic neurons, mostly in the pars compacta region of the substantia nigra, whereas MPTP-injected mice that received Mito-Q_{10} showed protection against MPTP toxicity (Fig. 6C).

Mito-Q_{10} improves locomotor activities in MPTP-treated mice

To investigate whether Mito-Q_{10} protects against structural and neurochemical damage as well as the functional impairments caused by MPTP, we monitored the locomotor activities in an open-field and rotarod experiment. The foot movements of control, MPTP-treated, and MPTP plus Mito-Q_{10}-treated mice were tested using a VersaMax infrared computerized activity monitoring system (AccuScan) and rotarod instrument (AccuScan) (Fig. 7). Representative maps (Versa-Plot) of the respective groups of mice are shown in Fig. 7A. We

found a marked decrease in the horizontal activity (Fig. 7B), vertical activity (Fig. 7C), total distance traveled (Fig. 7D), total movement time (Fig. 7E), and rearing activity (Fig. 7G) in MPTP-treated mice. The total rest time for MPTP-induced mice increased (Fig. 7F). As shown in these representations, Mito-Q_{10} treatment restored the behavioral parameters of MPTP-treated mice to the levels observed in control mice. At 20 rpm, MPTP-treated mice showed a decrease (>75%) in time spent on the rotarod compared to control mice. However, MPTP-injected mice that also received Mito-Q_{10} showed only a modest decrease (<25%) in the time spent on the rotarod compared to the levels observed in control mice (Fig. 7H). Collectively, these results generated from the behavioral tests demonstrate that Mito-Q_{10} protected against MPTP-induced loss of locomotor activities and foot movement.

Mito-Q_{10} pretreatment inhibits mitochondrial aconitase inactivation: ex vivo EPR measurements

Next we determined whether Mito-Q_{10} inhibits MPTP-induced oxidative damage in the mitochondria using an ex vivo EPR analysis. We used the EPR signal derived from inactivated aconitase as a marker of mitochondrial damage. Tissues isolated from the striatum and SN of mice treated with saline, MPTP, and MPTP plus Mito-Q_{10} were frozen in liquid nitrogen, transferred to EPR tubes, and analyzed at liquid helium temperatures. Fig. 8 shows the ex vivo low-temperature EPR spectra recorded at 10–15 K. As shown, MPTP treatment considerably increased the EPR signal intensity due to the $[3Fe–4\ S]^+$ cluster compared to control striatum (Fig. 8). Mito-Q_{10} treatment inhibited this increase in signal intensity, suggesting decreased oxidative damage. The EPR spectrum is characteristic of the $[3Fe–4\ S]^+$ cluster of inactive aconitase with distinctive absorptions in the g=2.03 and 2.01 regions [45,46]. Because of the spin-relaxation mechanism, this particular iron–sulfur center could be detected only at low temperatures. The same trend was noticed in the striatum and in the SN, although changes were more pronounced in SN. Further analysis of the expanded EPR spectrum (Figs. 8B and 8C) and comparison with the EPR spectra of authentic $[3Fe–4\ S]^+$ forms of cytosolic and mitochondrial aconitases suggest that the EPR spectrum obtained from brain tissues closely resembles the $[3Fe–4\ S]^+$ form of mitochondrial aconitase and not the cytosolic form of aconitase. As shown in Fig. 8C, distinctly different EPR spectra were obtained from pure cytosolic aconitase and mitochondrial aconitase enzymes. These results indicate that Mito-Q_{10} treatment mitigates MPTP-mediated inactivation of mitochondrial aconitase. Mito-Q_{10} also inhibits the increase in the EPR signal intensity at g=6 (attributed to cytochrome *c*) detected in brain tissues obtained from MPTP-treated mice.

Ex vivo EPR of SN and striatum tissues from MPTP/Mito-Q_{10}-treated mice: microwave power and temperature dependence

We measured the microwave power and temperature dependence of other Fe–S clusters in addition to aconitase. EPR spectra at various microwave powers ranging from 0.1 to 150 mW were used to investigate the alterations in structural and magnetic interactions surrounding the active metal centers after MPTP/Mito-Q_{10} treatment. The EPR power saturation curves for striatum tissue obtained from normal mice and from mice treated with MPTP are shown in Supplementary Fig. S1. The EPR spectra recorded from the striatum tissue of mice treated with Mito-Q_{10} plus MPTP were similar to those obtained from control

brain tissue (not shown). EPR relaxation profiles at g=6, 2.015, and 1.94 and saturation parameters were analyzed (see legend to Supplementary Fig. S1).

However, compared to g_x =2.015 and g_z =6, the power saturation line shapes of g_y =1.94 were not affected by MPTP treatment. This confirms the absence of any oxidative damage to complex I Fe–S clusters as monitored by EPR. The $P_{1/2}$ values of the g =6 signal were affected by MPTP treatment that was partially inhibited by Mito-Q_{10} (not shown). A twofold increase in the $P_{1/2}$ values of g =2.015 after MPTP treatment was observed, indicating the formation of new signal due to the mitochondrial aconitase (m-aconitase) [3Fe–4 S]$^+$ signal. Supplementary Fig. S1 shows the temperature-dependence EPR of the signals plotted as signal amplitude versus temperature at g_z =6, g_y =2.015, and g_x =1.94 for SN tissues of control (solid lines) and MPTP-treated mice. SN tissues of mice treated with Mito-Q_{10} plus MPTP were similar to those of control (not shown). It is evident that the high-spin heme signal is ferromagnetic. The temperature dependences of signals due to [3Fe–4 S]$^+$ were antiferromagnetically coupled. The temperature dependence of the signal at g=2.015 is typical of the behavior of a [3Fe–4 S]$^+$ cluster exhibiting high EPR signal intensity at 10 K and diminished to the basal level at 35 K. Above 35 K, the residual signal is only a small free radical at g=2.003. There was a dramatic increase in signal intensities at g=6 and g=2.015. However, the temperature variations of the g=1.94 signal (Supplementary Fig. S1) of SN tissue, SN tissue plus MPTP, and SN tissue plus Mito-Q_{10} and MPTP were not affected, suggesting the absence of any possible damage to iron–sulfur clusters associated with complex I.

Discussion

This study demonstrates that Mito-Q_{10} pretreatment protected against MPTP-induced behavioral deficits, TH-positive neuronal loss, depletion of striatal dopamine and DOPAC, inactivation of mitochondrial aconitase, and neuronal apoptosis and cell death. Supplementing MDNs with a mitochondria-targeted ubiquinone (Mito-Q_{10}) rescued the neurons from MPP^+-induced toxicity and related biochemical alterations.

Mitochondrial toxin-induced PD animal models

MPP^+, rotenone, and paraquat have been widely used as compounds that could induce biochemical changes and symptoms in animals that closely mimic those of human PD pathophysiology [47,48]. A substantial decrease in the levels of ubiquinone, an antioxidant and important cofactor in the mitochondrial electron transport chain, was detected in dopamine neurons during treatment with several parkinsonian mimetics [49,50]. Although a substantial decrease in complex I activity was reported in SN in brains affiicted by PD, in previous studies, a closer analysis indicated mitochondrial complex IV defects in PD [51]. The environmental neurotoxin MPTP recapitulates major biochemical and pathological findings of idiopathic PD. MPTP and other inhibitors of mitochondrial complex I activity induced phosphorylation of peroxiredoxin-2 (Prx2) and inhibition of Prx2 peroxidase activity. The loss of Prx2 peroxidase activity results in increased ROS levels in dopaminergic neurons [51].

Although the MPTP animal model is probably the best and only available drug-induced preclinical model, its relevance to idiopathic PD is still controversial. It is well known that the nigrostriatal dopaminergic neurons are substantially destroyed in PD in a slow and progressive manner. The MPTP model replicates many of the lesions of the nigrostriatal dopaminergic pathway, albeit with rapid nigral damage. Although several neurotoxins (6-hydroxydopamine or rotenone or paraquat) have been used to mimic PD in animal models, MPTP is the only dopaminergic neurotoxin that, in monkeys, induces clinical symptoms indistinguishable from idiopathic PD. The MPTP mouse model is an alternate reliable rodent model for investigating the effectiveness of MTAs in neuroprotection. Although the MPTP mouse model reliably mimics dopamine cell loss in the nigrostriatal dopamine circuit, this model does not, however, reproduce the pathology and cell loss that occur in other brain regions. In addition, this mouse model does not include nonmotor changes that occur in human PD. Despite these deficiencies, the MPTP model has been routinely used by many researchers to test the efficacy of new therapies for PD.

MTAs as neuroprotectants

As conventional ROS detoxification probes (vitamin E, tempol, ubiquinone) do not significantly accumulate within mitochondria, their ability to scavenge mitochondrial ROS/reactive nitrogen species (RNS) is limited. Antioxidants (vitamin E and Co-Q) coupled to a triphenylphosphonium cation accumulate in mitochondria [29,52,53]. Previous studies suggest that the intramitochondrial concentrations of MTAs can be 100- to 500-fold higher than the cytosolic levels [52,53]. The large negative membrane potential of 150–180 mV across the mitochondrial inner membrane potentiates the uptake and distribution of lipophilic cations from the intracellular space into the mitochondria [53]. A substantial decrease in the levels of Co-Q, an antioxidant and critical cofactor in the mitochondrial respiratory chain, was detected in Parkinson's animal models [49,50]. Supplementing MDNs with high levels of Co-Q or with a chemically modified, targeted Co-Q (i.e., Mito-Q_{10}), therefore, seemed a logical neuroprotective strategy. To our knowledge, the efficacy of MTAs in a preclinical in vivo animal model of PD is yet to be evaluated. The present data suggest that pretreatment with Mito-Q_{10} thwarts MPTP toxicity in cell culture and animal models. Mito-Q_{10} has been used as a neuroprotective agent in a mouse model of Friedreich ataxia (FRDA), an autosomal disease resulting from mutations in the FRDA gene encoding the mitochondria-targeted protein frataxin [54]. The ability of Mito-Q_{10} to function as an antioxidant was related to the redox reaction between the oxidized and the reduced forms of Mito-Q_{10} and ROS/RNS.

MTAs exert their antioxidant mechanism of action via several pathways. Mito-Q_{10}, a redox mixture of quinone and hydroquinone, undergoes reduction in the mitochondrial matrix to form the quinol form (reduced form), which is presumably the active form of the drug. The quinol form is oxidized back to quinone by ROS/RNS including lipid peroxyl radical, hydroxyl radical, superoxide, and peroxynitrite [55]. Whereas Mito-quinol reacts slowly with superoxide, Mito-quinone reacts rapidly with superoxide (k=5×10^8 M^{-1} s^{-1}). Mito-Q_{10} mainly reacts as Mito-quinol with lipid peroxidation intermediates [55–57]. Although MnSOD is highly abundant, cellular antioxidant systems including MnSOD are severely affected in neurological diseases [58].

The key issue in MTA-mediated antioxidant therapy is whether MTA exerts its protective action at the intended target (i.e., mitochondria). In this regard, monitoring the changes in the mitochondrial aconitase iron–sulfur cluster EPR signal in brain tissues provided an important mechanistic insight. As shown in Fig. 8, Mito-Q_{10} inhibited the formation of the $[3Fe–4\ S]^{+}$ cluster signal from mitochondrial aconitase. Inactivation of aconitase enzyme occurs as a result of superoxide-induced oxidation of the $[4Fe–4\ S]^{2+}$ cluster to a $[3Fe–4\ S]^{+}$ cluster. The $[4Fe–4\ S]^{2+}$ cluster present in the native aconitase enzyme is EPR silent, whereas the $[3Fe–4\ S]^{+}$ cluster is EPR active. The low-temperature EPR of the $[3Fe–4\ S]^{+}$ form of mitochondrial aconitase is distinctly different from that of the cytosolic aconitase. Because of the compensatory elevation in mitochondrial enzyme expression in MPTP-treated mice [59], the low-temperature EPR is the only method by which inactivation of mitochondrial iron–sulfur clusters can be monitored.

MTAs as potential therapeutics for PD treatment

The mitochondria-targeted antioxidant Mito-Q_{10} has undergone phase 1 and phase 2 clinical trials [60]. Daily oral doses of 40–80 mg Mito-Q_{10} prevent liver damage in hepatitis C patients [61]. However, in a recent limited clinical trial, year-long administration of Mito-Q_{10} to Parkinson’s disease patients did not alter disease progression [60]. In this study, prophylactic and continuous administration of Mito-Q_{10} afforded neuroprotection in MPTP-treated mice. Mito-$Q_{10\ was}$ administered before and after MPTP treatment. In humans, Mito-Q_{10} treatment was initiated after discovering the changes in the behavior of PD patients [60]. Additional consideration should be given to appropriate patient selection for neuroprotective trials. Thus, timing and dosing of Mito-Q_{10} administration in humans seem to be critical for successful management of PD. More recently, investigators showed that a water-soluble analog of coenzyme Q_{10} ameliorated the PD symptoms in rats exposed to paraquat treatment [62]. The experimental protocols involved pretreatment with water-soluble CoQ_{10}, before paraquat treatment. Clearly, these aspects (i.e., fortification of cells and tissues with MTA dosage and pretreatment) should be taken into consideration before designing appropriate clinical trials in humans or assessing the role of mitochondrial oxidative stress in PD pathogenesis.

Although the MPTP mouse model has been widely used as a potential preclinical model for PD, there are some caveats that need to be taken into consideration. The MPTP mouse model does not fully reflect the human PD pathology (e.g., inclusion formation) that is associated with chronic age-related processes. In this regard, it is important to elucidate the neuroprotective effect of MTAs such as Mito-Q in recently established genetic models of PD [63,64]. These genetic models mimic dopamine loss in the substantia nigra, as occurs in age-related PD in humans.

Supplementary Material

Refer to Web version on PubMed Central for supplementary material.

Acknowledgments

This work was supported by National Institutes of Health Grant R01 NS039958 (B.K., A.K.) and the Parkinson's Foundation (B.K.). The W. Eugene and Linda Loyd Endowed Chair to A.G.K. is also acknowledged. We thank Mr. Christopher Andrekopoulus, Ms. Sonya Cunningham, and Dr. Danhui Zhang for their technical assistance.

Abbreviations

DPBS	Dulbecco's phosphate buffered saline
EPR	electron paramagnetic resonance
MDN	mesencephalic dopamine neurons
Mito-Q_{10} or Mito-Q	ubiquinone (Co-Q_{10}) attached to triphenylphosphonium cation
MPP^+	1-methyl-4-phenyl pyridinium ion
MPTP	1-methyl-4-phenyl-1,2,3,6-tetrahydropyridine
MTA	mitochondria-targeted antioxidant
MTT	3-[4,5-dimethylthiazol-2-yl]-2,5-diphenylte-trazolium bromide
PD	Parkinson's disease
RNS	reactive nitrogen species
ROS	reactive oxygen species
SN	substantia nigra
TH	tyrosine hydroxylase

References

1. Burns RS, Chiueh CC, Markey SP, Ebert MH, Jacobowitz DM, Kopin IJ. A primate model of parkinsonism: selective destruction of dopaminergic neurons in the pars compacta of the substantia nigra by N-methyl-4-phenyl-1, 2, 3, 6-tetrahydropyridine. Proc Natl Acad Sci USA. 1983; 80:4546–4550. [PubMed: 6192438]
2. Dawson TM, Dawson VL. Molecular pathways of neurodegeneration in Parkinson's disease. Science. 2003; 302:819–822. [PubMed: 14593166]
3. Parker WD Jr, Boyson SJ, Parks JK. Abnormalities of the electron transport chain in idiopathic Parkinson's disease. Ann Neurol. 1989; 26:719–723. [PubMed: 2557792]
4. Fahn, S.; Przedborski, S. Parkinsonism. In: Rowland, LP., editor. Merritt's Neurology. Lippincott, Williams & Wilkins; New York: 2002. p. 679-695.
5. Greenamyre JT, Betarbet R, Sherer T, Panov A. Parkinson's disease, pesticides and mitochondrial function. Trends Neurosci. 2001; 24:247.
6. Jackson-Lewis V, Przedborski S. Protocol for the MPTP mouse model of Parkinson's disease. Nat Protoc. 2007; 2:141–151. [PubMed: 17401348]
7. Mizuno Y, Susuki K, Sone N, Saitoh T. Inhibition of mitochondrial respiration by 1-methyl-4-phenyl-1, 2, 3, 6-tetrahydropyridine in mouse brain in vivo. Neurosci Lett. 1988; 91:349–353. [PubMed: 3141846]
8. Langston JW, Ballard P, Tetrud JW, Irwin I. Chronic parkinsonism in humans due to a product of meperidine analog synthesis. Science. 1983; 219:979–980. [PubMed: 6823561]
9. Davis GC, Williams AC, Markey SP, Ebert MH, Caine ED, Reichert CM, Kopin IJ. Chronic parkinsonism secondary to intravenous injection of meperidine analogs. Psychiatry Res. 1979; 1:249–254. [PubMed: 298352]

10. Forno LS, DeLanney LE, Irwin I, Langston JW. Similarities and differences between MPTP-induced parkinsonism and Parkinson's disease: neuropathologic considerations. Adv Neurol. 1993; 60:600–608. [PubMed: 8380528]
11. Heikkila RE, Manzino L, Cabbat FS, Duvoisin RC. Protection against the dopaminergic neurotoxicity of 1-methyl-4-phenyl-1, 2, 5, 6-tetrahydropyrine by monoamine oxidase inhibitors. Nature. 1984; 311:467–469. [PubMed: 6332989]
12. Sherer TB, Betarbet R, Stout AK, Lund S, Baptista M, Panov AV, Cookson MR, Greenamyre JT. An *in vitro* model of Parkinson's disease: linking mitochondrial impairment to altered alpha-synuclein metabolism and oxidative damage. J Neurosci. 2002; 22:7006–7015. [PubMed: 12177198]
13. Chiba K, Trevor A, Castagnoli N Jr. Metabolism of the neurotoxic tertiary amine, MPTP, by brain monoamine oxidase. Biochem Biophys Res Commun. 1984; 120: 574–578. [PubMed: 6428396]
14. Ramsay RR, Kowa AT, Johnson MK, Salach JI, Singer TP. The inhibition site of MPP+, the neurotoxic bioactivation product of 1-methyl-4-phenyl-1, 2, 3, 6-tetrahydropyridine, is near the Q-binding site of NADH dehydrogenase. Arch Biochem Biophys. 1987; 259:645–649. [PubMed: 2827583]
15. Bates TE, Heales SJ, Davies SE, Boakye P, Clark JB. Effects of 1-methyl-4-phenylpyridinium on isolated rat brain mitochondria: evidence for a primary involvement of energy depletion. J Neurochem. 1994; 63:640–648. [PubMed: 8035188]
16. Schapira AH, Cooper VJM, Dexter D, Jenner P, Clark JB, Marsden CD. Mitochondrial complex I deficiency in Parkinson's disease. J Neurochem. 1990; 54: 823–827. [PubMed: 2154550]
17. Schapira AHV. Mitochondrial disease. Lancet. 2006; 368:70–82. [PubMed: 16815381]
18. Schmidt N, Ferger B. Neurochemical findings in the MPTP model of Parkinson's disease. J Neural Transm. 2001; 108:1263–1282. [PubMed: 11768626]
19. Jha N, Jurma O, Lalli G, Liu Y, Pettus EH, Greenamyre JT, Liu RM, Forman HJ, Andersen JK. Glutathione depletion in PC12 results in selective inhibition of mitochondrial complex I activity: implications for Parkinson's disease. J Biol Chem. 2000; 275:26096–26101. [PubMed: 10846169]
20. Lin MT, Beal FM. Mitochondrial dysfunction and oxidative stress in neurodegenerative diseases. Nature. 2006; 443:787–802. [PubMed: 17051205]
21. Schon EA, Manfredi G. Neurodeneration and mitochondrial dysfunction. J Clin Invest. 2003; 111:303–312. [PubMed: 12569152]
22. Betarbet R, Sherer TB, MacKenzie G, Garcia-Osuna M, Panov AV, Greenamyre JT. Chronic systemic pesticide exposure reproduces features of Parkinson's disease. Nat Neurosci. 2000; 3:1301–1306. [PubMed: 11100151]
23. Götz ME, Künig G, Riederer P, Youdim MB. Oxidative stress: free radical production in neural degeneration. Pharmacol Ther. 1994; 63:37–122. [PubMed: 7972344]
24. Qian ZM, Wang Q. Expression of iron transport proteins and excessive iron accumulation in the brain in neurodegenerative disorders. Brain Res Rev. 1998; 27: 257–267. [PubMed: 9729418]
25. Golden TR, Patel M. Catalytic antioxidants and neurodegeneration. Antioxid Redox Signaling. 2009; 11:555–570.
26. Kieburtz K. Issues in neuroprotection clinical trials in Parkinson's disease. Neurology. 2006; 66(10 Suppl 4):S50–S57. [PubMed: 16717252]
27. Kaur D, Yantiri F, Rajagopalan S, Kumar J, Mo JQ, Boonplueang R, Viswanath V, Jacobs R, Yang L, Beal MF, DiMonte D, Volitaskis I, Ellerby L, Cherny RA, Bush AI, Anderson JK. Genetic or pharmacological iron chelation prevents MPTP-induced neurotoxicity *in vivo:* a novel therapy for Parkinson's disease. Neuron. 2003; 37:899–909. [PubMed: 12670420]
28. Dhanasekaran A, Kotamraju S, Kalivendi SV, Matsunaga T, Shang T, Keszler A, Joseph J, Kalyanaraman B. Supplementation of endothelial cells with mitochondria-targeted antioxidants inhibit peroxide-induced mitochondrial iron uptake, oxidative damage, and apoptosis. J Biol Chem. 2004; 279:37575–37587. [PubMed: 15220329]
29. Murphy MP. Selective targeting of bioactive compounds to mitochondria *in vivo*. Trends Biotechnol. 1997; 15:326–330. [PubMed: 9263481]

30. Kelso GF, Porteous CM, Hughes G, Ledgerwood EC, Gane AM, Smith RA, Murphy MP. Prevention of mitochondrial oxidative damage using targeted antioxidants. Ann NY Acad Sci. 2002; 959:263–274. [PubMed: 11976201]

31. Cheung NS, Hickling YM, Beart PM. Development and survival of rat embryonic mesencephalic dopaminergic neurones in serum-free, antioxidant-rich primary cultures. Neurosci Lett. 1997; 233:13–16. [PubMed: 9324228]

32. Dreschel DA, Liang LP, Patel M. 1-Methyl-4-phenylpyridinium-induced alterations of glutathione status in immortalized rat dopaminergic neurons. Toxicol Appl Pharmacol. 2007; 220:341–348. [PubMed: 17395226]

33. Zhang D, Anantharam V, Kanthasamy A, Kanthasamy AG. Neuroprotective effect of protein kinase C delta inhibitor rottlerin in cell culture and animal models of Parkinson's disease. J Pharmacol Exp Ther. 2007; 322:913–922. [PubMed: 17565007]

34. Kaul S, Kanthasamy A, Kitazawa M, Anantharam V, Kanthasamy AG. Caspase-3 dependent proteolytic activation of protein kinase C delta mediates and regulates 1-methyl-4-phenylpyridinium (MPP^+)-induced apoptotic cell death in dopaminergic cells: relevance to oxidative stress in dopaminergic degeneration. Eur J Neurosci. 2003; 18:1387–1401. [PubMed: 14511319]

35. Kalivendi SV, Kotamraju S, Zhao H, Joseph J, Kalyanaraman B. Doxorubicin-induced apoptosis is associated with increased transcription of endothelial nitric-oxide synthase: effect of antiapoptotic antioxidants and calcium. J Biol Chem. 2001; 276: 47266–47276. [PubMed: 11579094]

36. Kalivendi SV, Cunningham S, Kotamraju S, Joseph J, Hillard CJ, Kalyanaraman B. Alpha-synuclein up-regulation and aggregation during MPP^+-induced apoptosis in neuroblastoma cells: intermediacy of transferrin receptor iron and hydrogen peroxide. J Biol Chem. 2004; 279:15240–15247. [PubMed: 14742448]

37. Ghosh A, Roy A, Liu X, Kordower JH, Mufson EJ, Hartley DM, Ghosh S, Mosley RL, Gendelman HE, Pahan K. Selective inhibition of NF-kappaB activation prevents dopaminergic neuronal loss in a mouse model of Parkinson's disease. Proc Natl Acad Sci USA. 2007; 104:18754–18759. [PubMed: 18000063]

38. Benner EJ, Mosley RL, Destache CJ, Lewis TB, Jackson-Lewis V, Gorantla S, Nemachek C, Green SR, Przedborski S, Gendelman HE. Therapeutic immunization protects dopaminergic neurons in a mouse model of Parkinson's disease. Proc Natl Acad Sci USA. 2004; 101:9435–9440. [PubMed: 15197276]

39. Ghosh A, Roy A, Matras J, Brahmachari S, Gendelman HE, Pahan K. Simvastatin inhibits the activation of p21ras and prevents the loss of dopaminergic neurons in a mouse model of Parkinson's disease. J Neurosci. 2009; 29: 13543–13556. [PubMed: 19864567]

40. Dessolin J, Schuler M, Quinart A, De Giorgi F, Ghosez L, Ichas F. Selective targeting of synthetic antioxidants to mitochondria: towards a mitochondrial medicine for neurodegenerative diseases? Eur J Pharmacol. 2002; 447:155–161. [PubMed: 12151007]

41. Chandran K, Aggarwal D, Migrino RQ, Joseph J, McAllister D, Konorev EA, Antholine WE, Zielonka J, Srinivasan S, Avadhani NG, Kalyanaraman B. Doxorubicin inactivates myocardial cytochrome c oxidase in rats: cardioprotection by Mito-Q. Biophys J. 2009; 96:1388–1398. [PubMed: 19217856]

42. Adams FS, La Rosa FG, Kumar S, Edwards-Prasad J, Kentroti S, Vernadakis A, Freed CR, Prasad KN. Characterization and transplantation of two neuronal cell lines with dopaminergic properties. Neurochem Res. 1996; 21:619–627. [PubMed: 8726972]

43. Clarkson ED, La Rosa FG, Edwards-Prasad J, Weiland DA, Witta SE, Freed CR, Prasad KN. Improvement of neurological deficits in 6-hydroxydopamine-lesioned rats after transplantation with allogeneic simian virus 40 large tumor antigen gene-induced immortalized dopamine cells. Proc Natl Acad Sci USA. 1998; 95:1265–1270. [PubMed: 9448320]

44. Doughan AK, Dikalov SI. Mitochondrial redox cycling of mitoquinone leads to superoxide production and cellular apoptosis. Antioxid Redox Signaling. 2007; 9: 1825–1836.

45. Vásquez-Vivar J, Kalyanaraman B, Kennedy MC. Mitochondrial aconitase as a source of hydroxyl radical: an electron spin resonance investigation. J Biol Chem. 2000; 275:14064–14069. [PubMed: 10799480]

46. Liang LP, Patel M. Iron–sulfur enzyme mediated mitochondrial superoxide toxicity in experimental Parkinson's disease. J Neurochem. 2003; 90:1076–1084. [PubMed: 15312163]
47. Gerlach M, Riederer P, Przuntek H, Youdim MB. MPTP mechanisms of neurotoxicity and their implications for Parkinson's disease. Eur J Pharmacol. 1991; 208: 273–286. [PubMed: 1815982]
48. Panov A, Dikalov S, Shalbuyeva N, Taylor G, Sherer T, Greenamyre JT. Rotenone model of Parkinson disease: multiple brain mitochondria dysfunctions after short term systemic rotenone intoxication. J Biol Chem. 2005; 280:42026–42035. [PubMed: 16243845]
49. Shults CW, Haas RH, Passov D, Beal MF. Coenzyme Q10 levels correlate with the activities of complexes I and II/III in mitochondria from parkinsonian and nonparkinsonian subjects. Ann Neurol. 1997; 42:261–264. [PubMed: 9266740]
50. Lovenberg W, Levine RA, Robinson DS, Ebert M, Williams AC, Calne DB. Hydroxylase cofactor activity in cerebrospinal fluid of normal subjects and patients with Parkinson's disease. Science. 1979; 204:624–626. [PubMed: 432666]
51. Przedborski S. Peroxiredoxin-2 links Cdk5 to neurodegeneration. Nat Med. 2007; 13: 907–909. [PubMed: 17680003]
52. Smith RAJ, Porteous CM, Coulter CV, Murphy MP. Selective targeting of an antioxidant to mitochondria. Eur J Biochem. 1999; 263:709–716. [PubMed: 10469134]
53. Smith RAJ, Porteous CM, Gane AM, Murphy MP. Delivery of bioactive molecules to mitochondria *in vivo*. Proc Natl Acad Sci USA. 2003; 100:5407–5412. [PubMed: 12697897]
54. Jauslin ML, Meier T, Smith RA, Murphy MP. Mitochondria-targeted antioxidants protect Friedreich ataxia fibroblasts from endogenous oxidative stress more effectively than untargeted antioxidants. FASEB J. 2003; 17:1972–1974. [PubMed: 12923074]
55. James AM, Cochemé HM, Smith RA, Murphy MP. Interactions of mitochondria-targeted and untargeted ubiquinones with the mitochondrial respiratory chain and reactive oxygen species: implications for the use of exogenous ubiquinones as therapies and experimental tools. J Biol Chem. 2005; 280: 21295–21312. [PubMed: 15788391]
56. Murphy MP, Smith RA. Targeting antioxidants to mitochondria by conjugation to lipophilic cations. Annu Rev Pharmacol Toxicol. 2007; 47:629–656. [PubMed: 17014364]
57. James AM, Sharpley MS, Manas A-RB, Frerman FE, Hirst J, Smith RAJ, Murphy MP. Interaction of the mitochondria-targeted antioxidant MitoQ with phospholipid bilayers and ubiquinone oxidoreductases. J Biol Chem. 2007; 282: 14708–14718. [PubMed: 17369262]
58. Schwartz JH, Tattersall I. Significance of some previously unrecognized apomorphies in the nasal region of *Homo neanderthalensis*. Proc Natl Acad Sci USA. 1996; 93:10852–10854. [PubMed: 8855270]
59. Kühn K, Wellen J, Link N, Maskri L, Lübbert H, Stichel CC. The mouse MPTP model: gene expression changes in dopaminergic neurons. Eur J Neurosci. 2003; 17: 1–12. [PubMed: 12534964]
60. Snow BJ, Rolfe FL, Murphy MP, Smith RA, Lockhart MM, Frampton CM, Taylor KM. Phase II study of the mitochondrial antioxidant mitoquinone for Parkinson's disease. Neurology. 2008; 70:A483–A484.
61. Gane EJ, Orr DW, Weilert F, Keogh GF, Gibson M, Murphy MP, Smith RAJ, Lockhart MM, Frampton CM, Taylor KM. Phase II study of the mitochondrial antioxidant mitoquinone for hepatitis C. J Hepatol. 2008; 48:S318.
62. Somayajulu-Nitu M, Sandhu JK, Cohen J, Sikorska M, Sridhar TS, Matei A, Borowy-Borowski H, Pandey S. Paraquat induces oxidative stress, neuronal loss in substantia nigra region and Parkinsonism in adult rats: neuroprotection and amelioration of symptoms by water-soluble formulation of coenzyme Q_{10}. BMC Neurosci. 2009; 10:88. [PubMed: 19635141]
63. Ekstrand MI, Terzioglu M, Galter D, Zhu S, Hofstetter C, Lindqvist E, Thams S, Bergstrand A, Hansson FS, Trifunovic A, Hoffer B, Cullheim S, Mohammed AH, Olson L, Larsson NG. Progressive parkinsonism in mice with respiratory-chain-deficient dopamine neurons. Proc Natl Acad Sci USA. 2007; 104: 1320–1325.
64. Lu ZH, Fleming SM, Meurers B, Ackerson LC, Mortazavi F, Lo V, Hernandez D, Sulzer D, Jackson GR, Maidment NT, Chesselet MF, Yang XW. Bacterial artificial chromosome transgenic mice expressing a truncated mutant parkin exhibit age-dependent hypokinetic motor deficits,

dopaminergic neuron degeneration, and accumulation of proteinase K-resistant α-synuclein. J Neurosci. 2009; 29:1962–1976. [PubMed: 19228951]

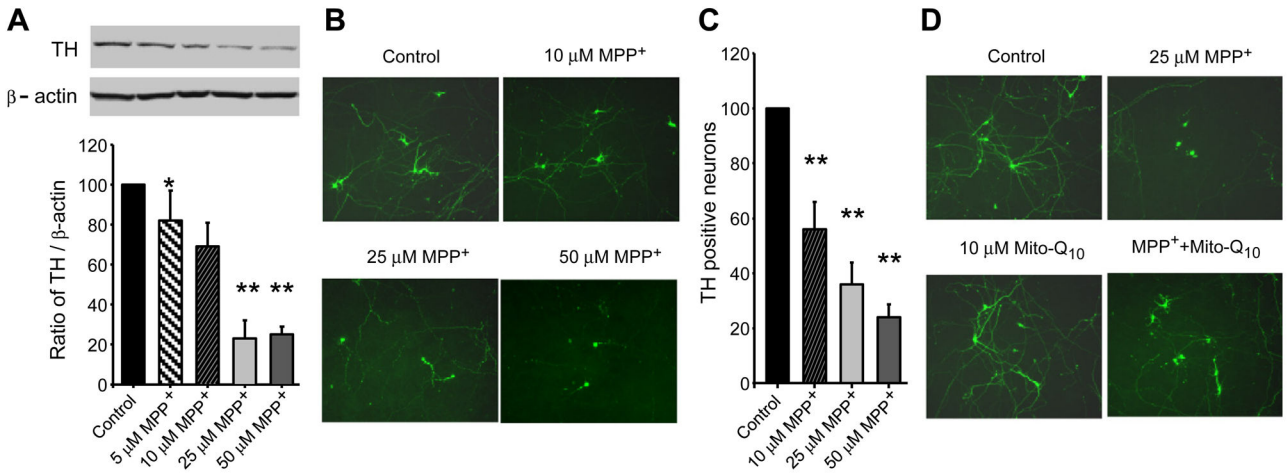

Fig. 1.

Inhibition of tyrosine hydroxylase protein in rat MDNs treated with MPP^+. (A) MDNs were treated with various concentrations of MPP^+ for 48 h, and the TH levels were determined by Western blotting using the monoclonal antibodies raised against TH and β-actin, followed by the secondary antibody coupled to horseradish peroxidase. Bands were visualized by an ECL detection system. The band intensities were calculated by densitometric analysis using Alpha Imager software, and the ratio of TH/β-actin was normalized to 100% in controls. (B) Under treatment conditions similar to those for (A), the survival of the dopamine neurons in cultures was visualized by immunocytochemistry using the polyclonal antibodies raised against TH and secondary antibody coupled to FITC. Fluorescence images were obtained using a Nikon fluorescence microscope equipped with Metamorph software. The numbers of surviving neurons with intact neurites were counted from 20 fields of view and the total numbers of neurons obtained in controls were normalized to 100%. (C) The densitometric analysis of the data shown in (B). (D) As described for (B), the survival of the dopamine neurons was visualized by immunohistochemistry. MDNs were treated with MPP^+, MPP^+ and Mito-Q_{10}, and Mito-Q_{10} for 48 h. Data shown are the means±SD of three separate experiments. $*P < 0.05$ and $**P<0.01$ compared to controls.

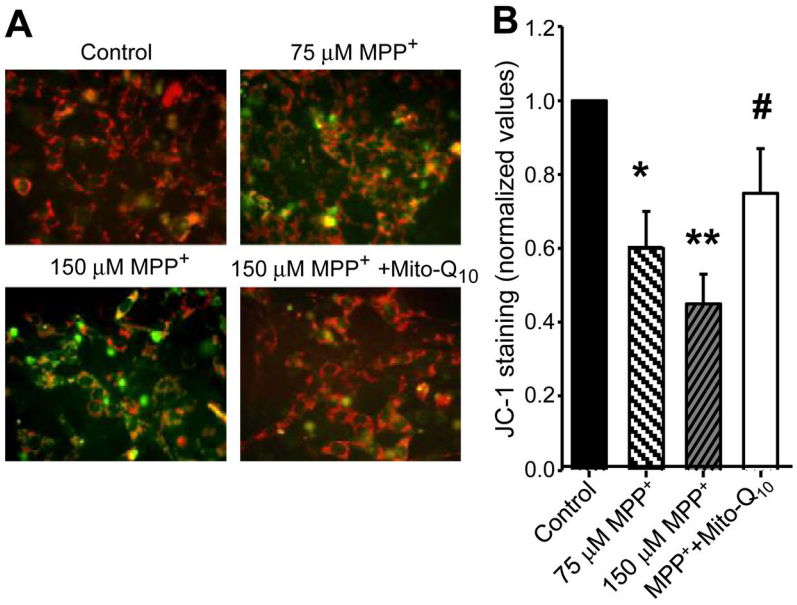

Fig. 2.

Mito-Q_{10} suppressed MPP^+-induced loss of mitochondrial membrane potential. (A) N27 cells were incubated with MPP^+ in the presence and absence of Mito-Q_{10} for 48 h. Cells were treated for 30 min with JC-1 (3 μl/ml) and washed twice with PBS, and the fluorescence images obtained under FITC and rhodamine filter settings were overlaid. (B) The number of cells demonstrating aggregated versus monomeric JC-1 probe was quantified by measuring the ratio between the fluorescence emission at 590 (orange) and 530 nm (green) in a Nikon fluorescence microscope using Metamorph software, and the values obtained under control conditions were normalized to 1. Data shown are the means±SD of three separate experiments. *P<0.05 and **P<0.01 compared to controls; #P<0.05 compared to MPP^+-treated group.

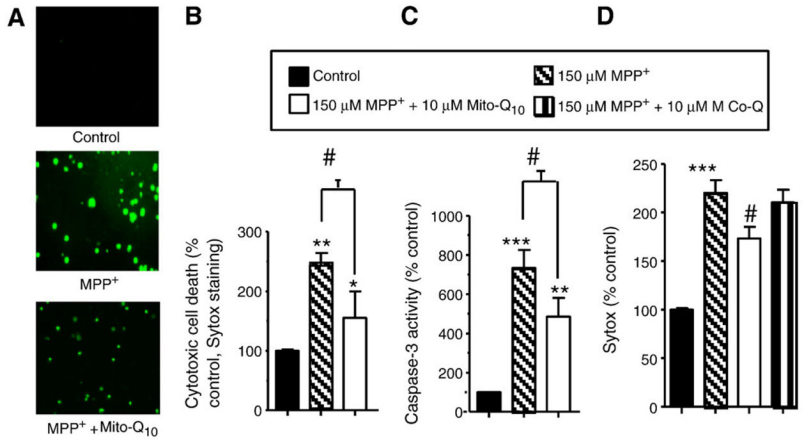

Fig. 3.

The protective effects of Mito-Q_{10} on MPP^+-induced toxicity in the rat N27 cell model. (A) N27 cells were treated with 150 μM MPP^+ in the presence and absence of Mito-Q_{10} for 48 h. The cytotoxicity was measured using the Sytox dye. (B) The densitometric results of the data shown in (A). (C) After the termination of incubation, caspase-3-like activity was measured in the cell lysate using the substrate DEVD-AFC as described under Materials and methods. (D) Same as (B) except that the effects of Mito-Q_{10} were compared with those of Co-Q. Data shown are the means±SD of four separate experiments. **P*<0.01 and ***P*<0.001, ****P*<0.0001 compared to controls; #*P*<0.001 compared to MPP^+-treated group.

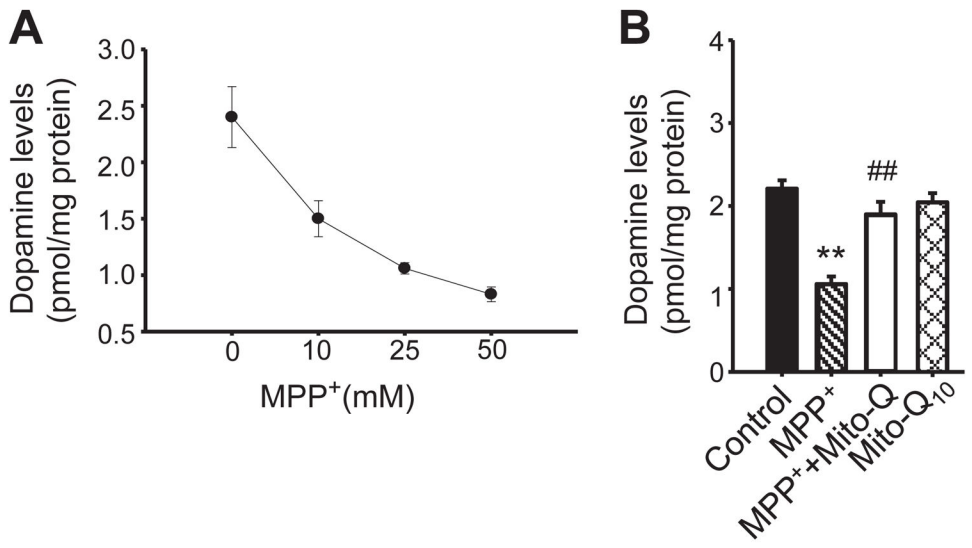

Fig. 4.

Pretreatment with Mito-Q_{10} restores dopamine levels in MPP^+-treated neuronal cells. (A) MDNs were treated with various concentrations of MPP^+. After the termination of incubation, the cells were washed three times with DPBS and lysed in 200 μl of 0.1 M perchloric acid. Dopamine levels were determined from 50-μl aliquots of clarified supernatant using an HPLC method with amperometric–CoulArray detection and a C18 reverse-phase column and TM-50 solvent (flow rate, 0.6 ml/min) as described under Materials and methods. Dopamine levels were normalized to the total protein and the values were calculated using the dopamine standard. (B) Dopamine levels were determined after treating MDNs with MPP^+ (25 μM), MPP^+ plus Mito-Q_{10}, and Mito Q. Data shown are the means±SD of three separate experiments. $^{**}P<0.01$ compared to controls; $^{\#}P<0.01$ compared to MPP^+-treated group.

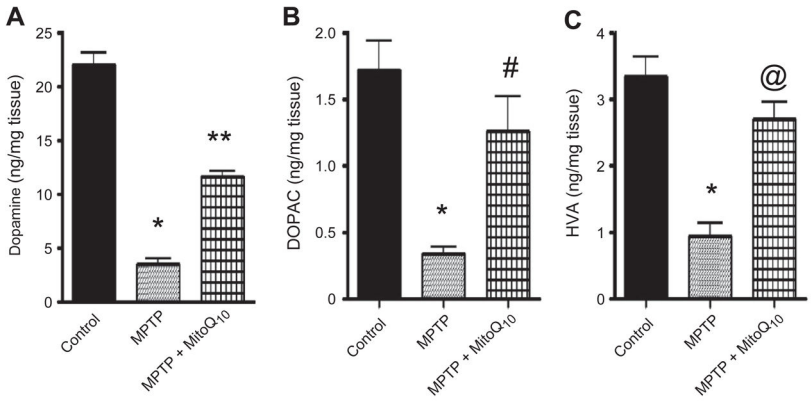

Fig. 5.

Effects of Mito-Q_{10} on the striatal dopamine and dopamine-derived metabolites in subacute MPTP-treated mice. Mice were administered Mito-Q_{10} (4 mg/kg) by oral gavage for 1 day (pretreatment before MPTP), 5 days (cotreatment with MPTP), and 7 days (posttreatment after MPTP). MPTP (25 mg/kg/day) was injected daily intraperitoneally for 5 days starting on day 2 and ending on day 7. Control mice received saline at the same dose. Seven days after the last MPTP injection, mice were sacrificed and (A) dopamine, (B) DOPAC, and (C) HVA were measured from striatum by HPLC. Data are means+SEM of six mice per group. *P<0.001 vs control; **P<0.001 vs MPTP; #P<0.05 vs MPTP; @P<0.01 vs MPTP.

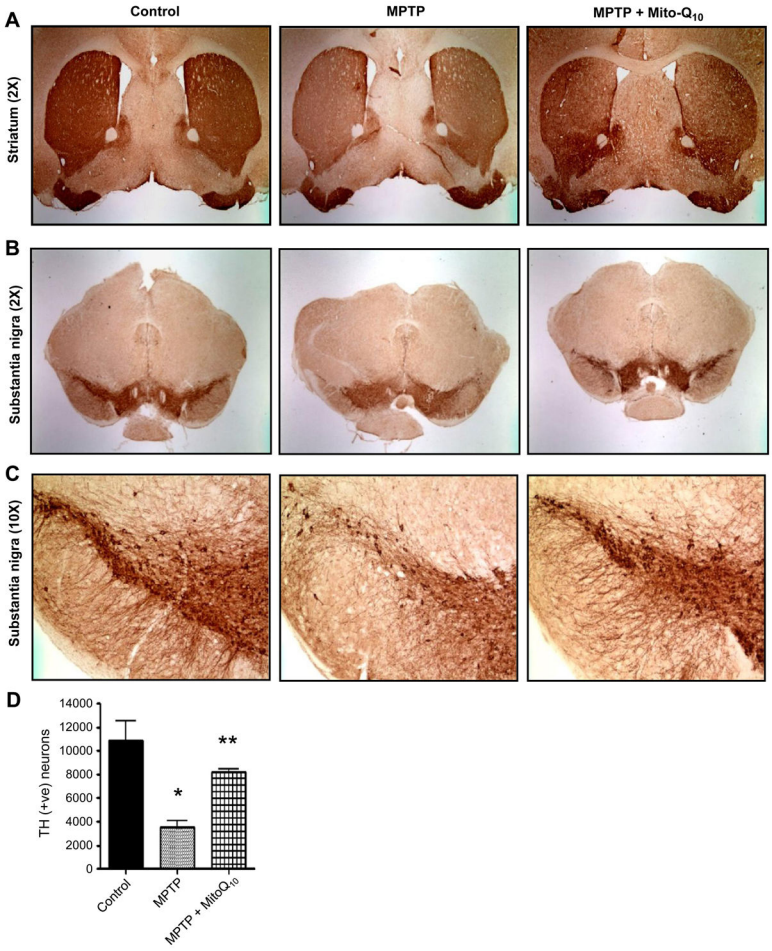

Fig. 6.

Effects of Mito-Q_{10} on nigrostriatum in subacute MPTP-treated mice. Mice were administered Mito-Q_{10} (4 mg/kg dose) by oral gavage for 1 day (pretreatment before MPTP administration), 5 days (cotreatment with MPTP), and 7 days (posttreatment after MPTP). MPTP (20 mg/kg) was administered intraperitoneally via a single dose daily starting on day 2 for 5 days. Control mice received saline at the same dose. Mice were perfused after 7 days of MPTP treatment and TH–DAB immunostaining was performed in (A) striatum (2× original magnification), (B) substantia nigra (2× original magnification), and (C) substantia nigra (10× original magnification). (D) Stereological counts of TH-positive neurons in the substantia nigra. Data are means±SEM of five or six mice per group; *P<0.01 vs control, **P<0.05 vs MPTP.

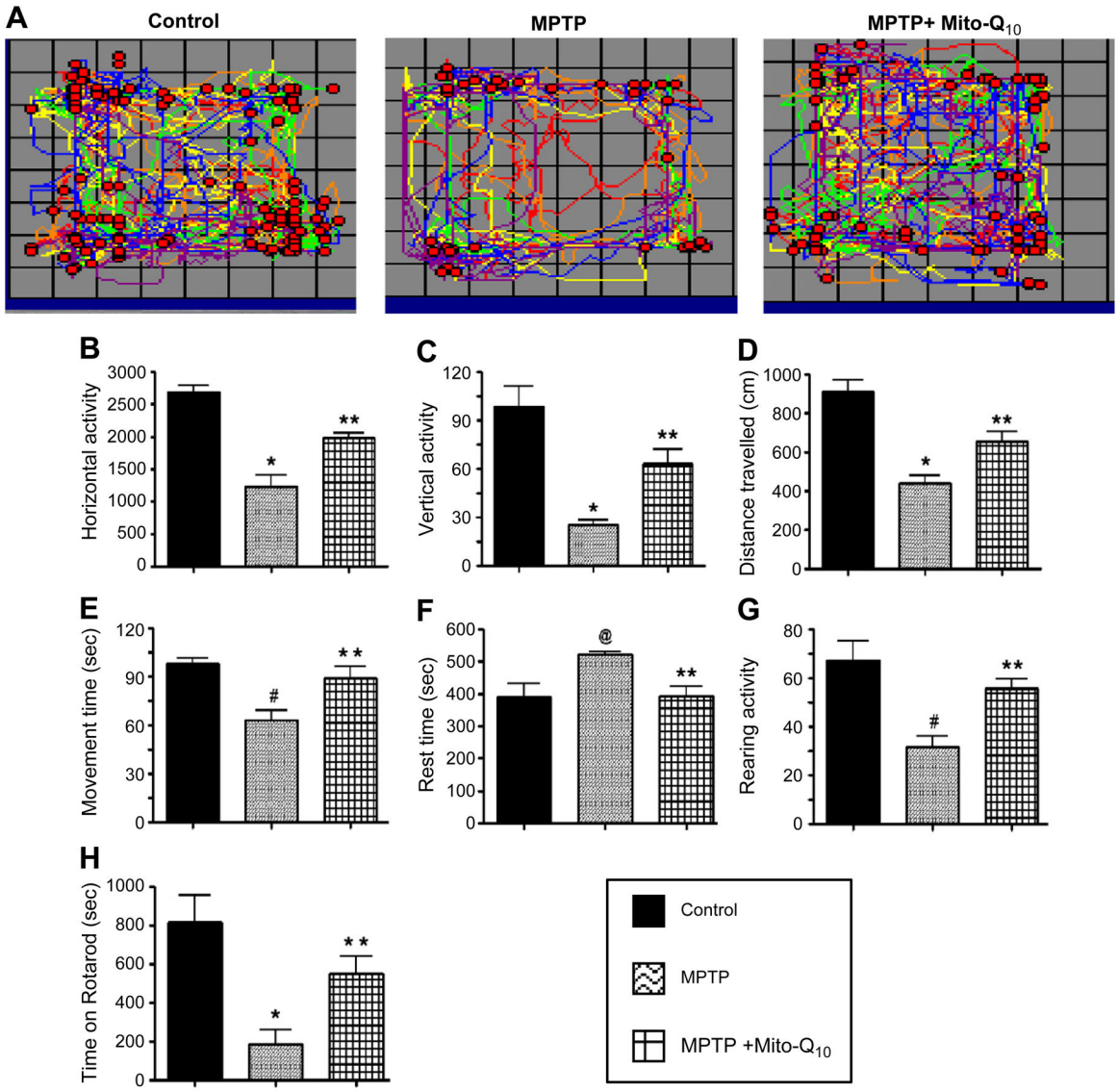

Fig. 7.

Effects of Mito-Q_{10} on MPTP-induced locomotor deficits. Mice were administered Mito-Q_{10} (4 mg/kg dose) by oral gavage for 1 day (pretreatment before MPTP administration), 5 days (cotreatment with MPTP), and 7 days (posttreatment after MPTP). MPTP (25 mg/kg) was administered at a single dose daily intraperitoneally starting on day 2 for 5 days. Control mice received saline at the same dose. The locomotor activities were measured using a VersaMax analyzer and rotarod, 5 days after the last MPTP injection. (A) Moving track of mice (VersaPlot); (B) horizontal activity; (C) vertical activity; (D) total distance traveled (cm); (E) total movement time (s); (F) total rest time (s); (G) rearing activity; (H) time spent on rotarod (s) at 20 rpm. Data are means+SEM of eight mice per group. *P<0.001 vs control; **P<0.05 vs MPTP; #P<0.01 vs control; @P<0.05 vs control.

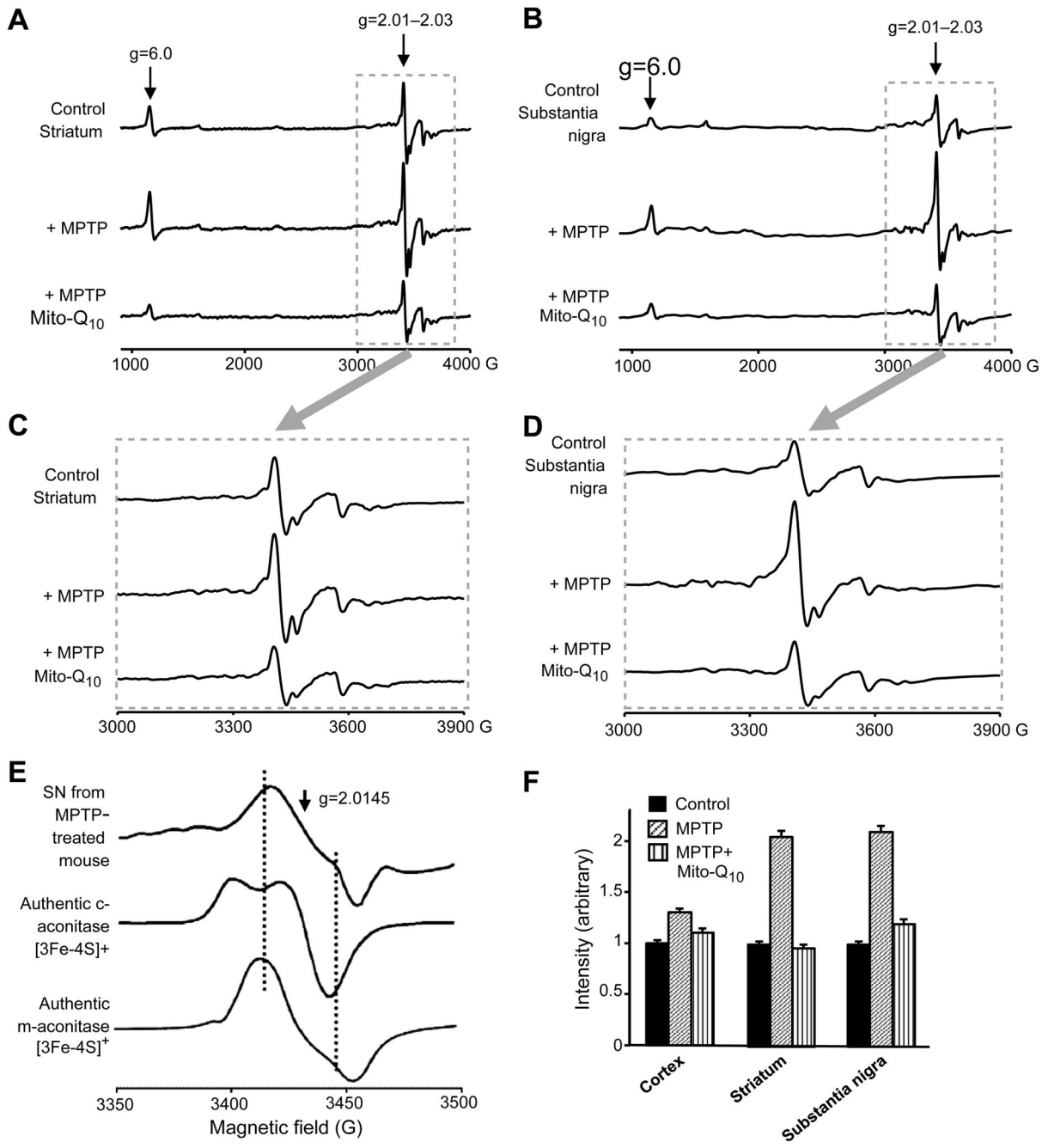

Fig. 8.

The low-temperature EPR spectra from mouse brain tissues. (A) EPR spectra were obtained at 10–15 K from striatal tissues isolated from MPTP- and MPTP plus Mito-Q_{10}-treated mice. (B) Same as (A), except that tissues were isolated from the substantia nigra of mice. (C) Expansion of the region inside the box shown in (A). (D) Expansion of the region inside the box shown in (B). (E) EPR spectra of authentic $[3Fe–4\ S]^+$ generated from cytosolic and mitochondrial aconitases. For the sake of comparison, the expanded spectrum at the region g=2.01–2.03 obtained from the SN tissues isolated from MPTP-treated mice is included. (F)

Bar graphs showing the spectral intensities of the signal obtained at g=2.01–2.03 from tissues isolated from the various regions of the brain from mice treated with MPTP and MPTP plus Mito-Q_{10}. Spectra were recorded at 10 K.